Plumage development and environmental factors influence surface temperature gradients and heat loss in wandering albatross chicks

David W. Stone[1,*], Carrie Gunn[2], Andreas Nord[1,3], Richard A. Phillips[2], Dominic J. McCafferty[1]

[1] *Scottish Centre for Ecology and the Natural Environment, Institute of Biodiversity, Animal Health and Comparative Medicine, College of Medical, Veterinary and Life Sciences, University of Glasgow, Rowardennan, G63 OAW, UK*

[2] *British Antarctic Survey, Natural Environment Research Council, High Cross, Madingley Road, Cambridge, CB3 0ET, UK*

[3]*Department of Biology, Section for Evolutionary Ecology, Sölvegatan 37, Lund University, SE-223 62, Lund, Sweden*

* Corresponding author: David W. Stone (david.stone.2@glasgow.ac.uk)

Abstract

Young birds in cold environments face a range of age-specific thermal challenges. Studying the thermal biology of young birds throughout ontogeny may further our understanding of how such challenges are met. We investigated how age and environmental parameters influenced surface temperature gradients across various body regions of wandering albatross (*Diomedea exulans*) chicks on Bird Island, South Georgia. This study was carried out over a 200 d period during the austral winter, from the end of the brood-guard period until fledging, bridging a gap in knowledge of surface temperature variation and heat loss in developing birds with a long nestling stage in severe climatic conditions. We found that variation in surface temperature gradients (i.e., the difference between surface and environmental temperature) was strongly influenced by chick age effects for insulated body regions (trunk), with an increase in the surface temperature gradient that followed the progression of plumage development, from the second set of down (mesoptiles), to final chick feathers (teleoptiles). Environmental conditions (primarily wind speed and relative humidity) had a stronger influence on the gradients in uninsulated areas (eye, bill) than insulated regions, which we interpret as a reflection of the relative degree of homeothermy exhibited by chicks of a given age. Based on biophysical modelling, total heat loss of chicks was estimated to increase linearly with age. However, mass specific heat loss decreased during the early stages of growth and then subsequently increased. This was attributed to age-related changes in feather growth and activity that increased surface temperature and, hence, metabolic heat loss. These results provide a foundation for further work on the effects of environmental stressors on developing chicks, which are key to understanding the physiological responses of animals to changes in climate in polar regions.

Keywords: thermoregulation; *Diomedea exulans*; development; climate; thermal imaging; polar; Antarctic.

1. Introduction

The ability of animals to survive in a harsh climate depends on their capacity for effective thermoregulation (Wharton 2002). Birds and mammals in polar regions possess a suite of morphological, behavioural and physiological attributes that allow them to live at environmental extremes (Blix 2016). For example, male emperor penguins (*Aptenodytes forsteri*) in Antarctica reduce their body surface area exposed to the environment by aggregating in tight, slowly-moving huddles as a behavioural strategy to minimise heat loss during incubation in the austral winter (Gilbert et al. 2006; 2007). Seabirds also reduce heat loss in cold environments through local heterothermy, whereby their extremities are allowed to cool almost to ambient with a concomitant preservation of core temperature (Irving & Krog 1955; Ponganis et al. 2003). Dense plumage is also an effective trait through which seabirds can physically limit heat loss and wetting in polar regions and elsewhere (Johansen & Bech 1983; Blix 2016; Osvath et al. 2018).

Nestling birds in polar regions cannot use the full suite of physiological and morphological adaptations available to adults for defending against the cold, and also face a range of age-specific thermal challenges that may affect their thermoregulatory costs. For example, juvenile birds have a larger surface area to volume ratio than adults and are therefore susceptible to higher rates of heat loss at a young age (Ricklefs 1989; Visser 1998). Initially, parents in surface-nesting seabird species provide protection against the elements by brooding their offspring for days or weeks after hatching. In most species, this is followed by several weeks or months when the parents still provision the chick, but it has to maintain its own temperature despite changes in the thermal environment. The development of endothermy, while concurrently ensuring optimal growth rate, requires effective management and allocation of resources (Ricklefs 1979; 1989). To offset some initial thermoregulatory costs, chicks of many seabirds hatch with natal down feathers that provide insulation from low air temperature

and wind; conditions which are often extreme at high-latitude nesting sites (Bostwick 2016). Rapid maturation of leg muscles throughout early development contributes to the chick's heat-producing capacity, because they are the main site of shivering thermogenesis in juveniles of this group of birds (Visser & Ricklefs 1995; Phillips & Hamer 2000). Simultaneous growth of the visceral organs, particularly the heart, lungs and liver, contribute to the ontogeny of endothermy by provision of oxygen and oxidative substrates to the muscles (Price & Dzialowski 2018). In addition, the steady postnatal development of the kidneys and gut facilitates digestion and processing of food, which supports the synthesis of structural tissue and growth of the second set of down (mesoptiles), followed by the final juvenile feathers (teleoptiles) (Phillips & Hamer 2000). Little is known about changes in thermoregulatory demands during this long process of development, and particularly about the role of plumage in providing much-needed insulation, particularly in extreme environments.

Surface temperatures are controlled by peripheral blood circulation and body insulation, but both insulated and non-insulated regions are affected by a range of environmental parameters including air temperature, wind speed, humidity and solar radiation (McCafferty et al. 2015; Gardner et al. 2016). The role of chick down as a highly effective insulation is highlighted in studies across a range of species including gentoo (*Pygoscelis papua*) and chinstrap (*Pygoscelis antarctica*) penguins (Visser 1998), and Laysan (*Phoebastria immutabilis*) and black-footed (*Phoebastria nigripes*) albatrosses (Howell & Bartholomew 1961). The uninsulated surface of the avian bill is recognised as a prominent 'thermal window', with control of blood flow in the vessel network below the keratinized surface regulating the extent to which heat is transferred to the environment (Symonds & Tattersall 2010; Schraft et al. 2019; Winder et al. 2020). Similarly, the un-feathered periorbital skin around the eye makes this a potentially important site for heat dissipation (Midtgård 1983; Buchholz 1996). Measuring surface temperatures of different body regions during ontogeny may, therefore, help

further our understanding of the thermal biology of young birds, how this is influenced by the nesting environment, and the extent to which their body surface temperature responds to environmental stressors.

Like many seabirds, the wandering albatross (*Diomedea exulans*) occupies an intermediate position on the altricial-precocial spectrum (Starck & Ricklefs 1998). The semi-altricial chicks hatch around mid-March following an incubation period of ~80 days, with both parents alternating brooding for a period lasting 21-43 days (Teixeira et al. 2014). The bulk of chick-rearing (post-brood period) occurs during the austral winter, during which time the chick is fed every few days and has to endure challenging environmental conditions including low temperatures (<-5°C) and high wind speeds (>60 km/h) (Ovstedal & Lewis-Smith 2001). Our study explored the extent to which surface temperature gradients (i.e., the difference between body surface and environmental temperatures) of different body regions (trunk, eye, head and bill) in wandering albatross chicks varied with age and plumage development, and in relation to environmental variables (wind speed, relative humidity and cloud cover). The rate of heat loss, and therefore the overall thermal challenge faced by an organism, increases when the gradient between the surface temperature and the environment increases, therefore, we predicted that: 1) chicks covered in down would exhibit lower surface temperature gradients in the trunk and head area, compared with uninsulated regions; 2) surface temperature gradients in insulated regions would increase with chick age, reflecting plumage development; 3) chicks would exhibit a decreasing surface temperature gradient with age in uninsulated regions (eye, bill); 4) surface temperature gradients would increase with increasing wind speed, relative humidity and cloud cover (indicative of poor weather) and these effects would be more pronounced in uninsulated regions. Finally, we modelled changes in metabolic heat loss of chicks throughout development to examine how age-related changes in surface temperature affected energy balance.

2. Materials and methods

2.1 Study site

Fieldwork was carried out on Bird Island, South Georgia (54° 00′ S, 38° 03′ W), southwest Atlantic Ocean (Fig. 1) between 21 April 2017 and 23 March 2018. South Georgia forms part of the subantarctic tundra biome, and the primary vegetation types in the region include subantarctic shrubs and herbs, grassland, ferns and clubmoss (Strother et al. 2015). The climate in this region is subpolar, with temperatures on the main island ranging from -19°C to +24°C (Davenport & Macalister 1996). Precipitation ranges from 1400-1800 mm annually, falling both as summer rain and several metres of snow during the winter (Ovstedal & Lewis-Smith 2001).

2.2 Data collection

An E300 FLIR thermal camera (FLIR Systems Inc, Oregon, USA) was used to record surface temperatures (^{o}C) of 20 known-age wandering albatross chicks at c. 2 week intervals. Chicks were monitored from the end of the brood-guard period until fledging, and ranged in age from 32-47 days old at the first session to a maximum of 377 days old at the end of the study. One chick failed to fledge as a result of a deformed wing and was subsequently removed from all analyses. Thermal images were taken on overcast days (i.e. avoiding direct sunlight), and not during periods of heavy rain or high winds as these factors are known to affect the reliability of surface temperature measurements when using infrared thermography (Cilulko et al. 2012). Timing of data collection was standardised to 14:00 GMT (solar noon) ± 2 hours to minimise effects of any circadian patterns in body temperature. A minimum of three full-frame side-profile thermal images and one regular photograph (as a record of plumage development/wetness) were taken from distances of 1-4 m. The distance from the camera to

the chick was measured to the nearest 10 cm using a laser distance meter (Leica Disto Classic, Leica Geosystems; St. Gallen, Switzerland). Air temperature (°C), relative humidity (%) and maximum wind speed (m/s) at the mean height of the chick above ground level were recorded using a hand-held meter (Kestrel 300, Kestrel Instruments; Pennsylvania, USA). Solar radiation has a strong influence on surface temperature (McCafferty et al. 2011; Cilulko et al. 2012), and therefore cloud cover (as % of obscured sky) was recorded as a proxy for solar radiation intensity (Matuszko 2012). After the images were taken, the chick was lifted onto a weighing platform placed alongside the nest and weighed to the nearest 10 g. Bill length and minimum bill depth were measured to the nearest 0.1 mm, and maximum wing chord recorded to the nearest 1.0 mm. Chicks were sexed (12 females, 7 males) using a discriminant function from bill length and depth measured at 260 days of age (British Antarctic Survey, unpublished data). There was no effect of sex on development of surface temperature gradients in any of the regions of interest, and sexes were therefore pooled in all analyses.

2.3 Image analysis

A total of 1033 thermal images of the 19 chicks that fledged were recorded over 25 sessions. The best quality image of each individual during each session in terms of image sharpness and the angle of the animal relative to the camera was used in further analyses. Good-quality images were unavailable from one session (29 July, 2017) due to a camera malfunction. A total of 357 images were therefore analysed using FLIR ThermaCAM Researcher Pro 2.10 (FLIR Systems Inc, Oregon, USA). Images were automatically adjusted using the Object Parameter Fields to account for variation in air temperature, relative humidity, distance (m), and emissivity of 0.98 (Hammel 1956). Reflected temperature and external optics temperature were assumed to equal air temperature. Posture potentially contributes to the extent of heat loss (Tickle & Codd 2019); therefore, each image was classified as standing or sitting. A five-level

plumage classification was applied, based on the percentage cover of juvenile (teleoptile) plumage, to describe the longitudinal change in plumage with chick age (Fig. 2). These values ranged from 0%, indicating full coverage of down, up to >75%, indicating a chick which had less than 25% of down remaining. Eye, bill, head and trunk (i.e., the main body of the chick, separate from the head) temperatures were obtained by fitting polygons and ellipses around the individual regions of interest; temperature values were then extracted from within the fitted shapes (Fig. 3).

2.4 Heat Transfer Modelling

Metabolic heat loss of chicks was estimated by calculating heat transfer rate by radiation and convection using measurements of surface temperature, assuming that the body of the chick could be approximated by a sphere (McCafferty et al. (2011).

2.4.1 Mean surface temperature of chicks

The mean surface temperature $\overline{T}_s$ (^{o}C) of a chick was determined by weighting the surface temperature of each region of interest (ROI: bill, head and trunk) according to the proportional area of the body part. Thermal images from a sample of five chicks at 4-week intervals (n=42) were selected to determine how the relative area of each ROI changed with age. Each area was determined by drawing a polygon around the ROI using the ImageJ 1.53a software (Schneider et al. 2012). A line was drawn along the bill and scaled according to the field measurements of bill length (mm) for each chick. This scaling was then used to derive the area of the ROI (m^2) and was then used to determine the proportional area of each ROI by dividing its area by the total area of all three body-parts. The diameter of the trunk (m) of the chick was determined by fitting a horizontal line through the centre of the trunk and scaled as above. The relationship between the proportional area of each ROI and chick age was modelled

using a linear mixed model with age as an explanatory variable and chick ID as a random effect (see details on packages and functions used in the Statistical Analysis section below). The proportional area of the bill and trunk did not vary with age (P>0.10 in both cases) but although significant (P=0.04) there was a minor change in the proportional area of the head (estimate = -6.6 x 10^{-5}) with age. As a simplification we therefore assumed that the proportional areas of the bill (0.03), head (0.09) and trunk (0.88) remained constant with age. Trunk diameter was then modelled with log age (P<0.001), and we then used this relationship to scale measurements for the heat loss model (trunk diameter = 17.8 × log(age) - 34.9).

2.4.2 Radiative heat loss

Radiative heat loss q_{rad} (W) was determined by solving the radiation balance at the surface. Heat loss by radiation was the difference between radiation emitted from the surface, q_{chick} and radiation gained from the environment, q_{env} such that:

$$q_{rad} = q_{chick} - q_{env} \quad (1)$$

where:

$$q_{rad} = A[\varepsilon\sigma(\overline{T}_s{}^4 - \overline{T}_{env}{}^4)] \quad (2)$$

where ε is blackbody emissivity (0.98), σ is the Stefan-Boltzmann constant (5.67 × 10^{-8} $Wm^{-2}K^{-1}$), and $\overline{T}_s$ and T_{env} are surface and environmental temperature (both in K), and A is total surface (m^2). We assumed that the chick exchanged radiation equally with the sky, such that $\overline{T}_{env}$ was taken to be the mean radiative temperature of the sky, T_{sky}, and surrounding air temperature, T_{air}. T_{sky} was dependent on cloud cover, such that when cloud cover was >50% or ≤50%, the effective T_{sky} was assumed to be 10°C and 20°C below air temperature, respectively (Monteith & Unsworth 1990).

2.4.3 Convective heat loss

Heat transfer by convection, q_{conv} (W) from the chick was estimated by:

$$q_{conv} = hA(\overline{T}_s - T_{air}) \quad (3)$$

Forced convection was assumed to dominate when wind speed u >0.1 ms^{-1} , such that the heat transfer coefficient h (Wm^{-2} ^{o}C^{-1}) was determined by:

$$h = Nu\frac{k}{d} \quad (4)$$

where k is the thermal conductivity of air (0.0243 Wm^{-1o}C^{-1} at 0^{o}C), *d (m*) is the characteristic dimension (i.e., body diameter; as above) and *Nu* is the dimensionless Nusselt number. The empirical relationship between *Nu* and the dimensionless Reynolds number *Re* was used for a sphere (Monteith & Unsworth 1990) where Re is calculated by:

$$Re = ud/v, \quad (5)$$

where v is the kinematic viscosity of air (1.33 × 10^{-5} m^{2}s^{-1} at 0^{o}C).

When wind speed was ≤0.1 ms^{-1}, we assumed free convection was dominant and therefore the heat transfer coefficient was determined according to the empirical relationship between the *Nu* and dimensionless Grashof Gr number for a sphere (Monteith & Unsworth 1990), and calculated as:

$$Gr = agd(\overline{T}_s - T_{air})/v^2 \quad (6)$$

where a is the coefficient of thermal expansion of air (3.7 × 10^{-3} K^{-1}) and acceleration of gravity, g (9.81 ms^{-2}).

The total heat loss (W) for the chick was estimated by summing the radiative and convective components. This was also expressed as heat flux (Wm^{-2}) and mass specific heat loss (Wkg^{-1}).

2.5 Statistical analysis

All statistical analyses were performed using R 3.5.1 for Windows (R Development Core Team 2018). As surface temperatures were strongly correlated with air temperature, we determined the temperature gradient between the air and the maximum surface temperature in the eye region, and the mean surface temperature in the trunk, bill and head regions. We created four candidate linear mixed-effects models (lmer function from the lme4 package) (Bates et al. 2015) to investigate the factors affecting chick surface temperatures across the eye region, trunk, bill and head. Chick age, posture, wind speed, relative humidity (as a proxy for days when rain had occurred) and cloud cover were set as fixed effects. To account for non-linear changes in surface temperature gradients throughout chick development, we also included age^2 as a covariate. The two-way interactions "age × wind speed", "age × relative humidity" and "age × cloud cover" were included in each candidate model to account for any age-related effects on the extent to which environmental factors affect chick surface temperatures. Similarly, we included the two-way interactions "age^2 × wind speed", "age^2 × relative humidity" and "age^2 × cloud cover" to account for any non-linear effects of age on the extent to which environmental factors affect chick surface temperatures.

Individual ID was included as a random effect (intercept) in all models. We assessed collinearity between independent predictor variables prior to analysis using variance inflation factors (vif function from the car package) (Fox & Weisberg 2011) and Spearman's rank correlation tests (cor function from the R base package) (R Development Core Team 2018). All variables analysed within each model had Spearman's rho <0.6 and VIF <2 (Zuur et al. 2007). Where a high level of correlation (Spearman's rho >0.6) was found between variables, one was discarded from the analysis. This only applied to the correlation between chick mass and chick age (Spearman's rho 0.72), and as the effects of the chick's age on surface temperature gradients was a primary focus of this study, chick mass was excluded from the analyses. Final models were derived through sequential exclusion of model terms with the

highest *P*-value starting with the highest order interactions, followed by a comparison of the complex and the reduced models (fitted with maximum likelihood) using likelihood ratio tests, retaining the parameters for which $P<0.05$. The final models were then re-fitted using restricted maximum likelihood, and degrees of freedom calculated using the Satterthwaite approximation method (lmerTest package) (Kuznetsova et al. 2017).

3. Results

3.1 Surface temperatures and environmental variables

Variation in absolute chick surface temperatures, surface-to-air temperature gradients, and environmental variables are given in Table 1. Absolute surface temperatures in uninsulated regions ranged from 11.6 to 31.5°C (eye) and 1.1 to 26.9°C (bill), whereas absolute surface temperature values in insulated regions ranged from -1.5 to 18.8°C (head) and -5.0 to 25.2°C (trunk) (n=357 observations of 19 individuals). Air temperature ranged from -5.1 to 9.3°C during the study. Throughout the study period, wind speeds of 0 – 14 m/s were recorded, and relative humidity of 54 – 100%. Cloud cover (% of obscured sky), used as a proxy for solar radiation intensity, ranged from 10 – 100%, with a mean of ~82%.

3.2 Age effects

There was a highly significant non-linear increase in the trunk surface temperature gradient with chick age ($P=0.0006$) (Fig. 4; Fig. 5c; Table 2), which followed the gradual change in plumage from down to teleoptile (juvenile) feathers which begins when chicks reach 100-120 days of age (Fig. 4; Fig. 5b; Table 2). In contrast, the eye region surface temperature gradient showed a highly significant decrease as chicks aged ($P<0.0001$), particularly from 100-120 days of age onwards (Fig. 4; Fig. 5e; Table 2). The bill surface temperature gradient also decreased with chick age ($P=0.001$) (Fig. 4; Fig. 5f; Table 2). There was no significant

effect of chick age on the head surface temperature gradient (P=0.55) (Fig. 4; Fig. 5d; Table 2).

3.3 Environmental effects

The extent to which wind speed, relative humidity and cloud cover affected the eye region surface temperature gradient was dependent on the age of the chick. There were significant two-way interactions between "age × wind speed" (P=0.04), "age × relative humidity" (P=0.004) and "age × cloud cover" (P=0.01), with wind speed, relative humidity and cloud cover appearing to have less of an effect on the eye region surface temperature gradient as chicks aged (Fig. 6; Table 2). Trunk (P=0.005) and head (P=0.002) surface temperature gradients decreased significantly with increasing wind speed (Fig. 7; Table 2). The bill surface temperature gradient decreased with increasing relative humidity (P< 0.0001) and with increasing cloud cover (P=0.04) (Fig. 7; Table 2). The effect of relative humidity and cloud cover varied with age for trunk (age × relative humidity: P=0.04; age × cloud cover: P=0.02) and head (age × relative humidity: P=0.02; age^2 × cloud cover: P=0.006) surface temperature gradients. However, variation was not uniform across different age categories (Fig. S1; Table 2).

3.4 Heat loss of chicks

Total heat loss of chicks was estimated to increase with age, ranging from around 10 W to over 30 W from 40 to 250+ days of age (Fig. 8a). The corresponding heat flux showed a different pattern, with relatively constant heat flux of around 40 Wm^{-2} from 40-150 days of age, followed by an increase to ~100 Wm^{-2} prior to fledging (Fig. 8b). In contrast, the mass specific heat loss (Wkg^{-1}) decreased during the early stages of development from around 2.5

to 1.5 Wm^{-2} at ~150 days of age and then increased to ~3.5 Wkg^{-1} close to fledging (Fig. 8c), corresponding to the similar trend in mean surface temperature (Fig. 8d).

4. Discussion

Our results suggest that changes in the plumage during development when chicks are transitioning between down and the final juvenile feathers (teleoptiles) were an important determinant of the variation in surface temperature gradients across different body regions. We also show that weather conditions are key factors influencing surface temperature gradients, with increasing wind speed, cloud cover and relative humidity resulting in lower surface temperatures in chicks. There was evidence in support of our hypothesis that downy chicks exhibit lower surface temperatures in the well-insulated trunk region prior to the transition to juvenile plumage, which starts at 100-120 days of age (Fig. 5b). This suggests that natal down acts as a very effective insulator from cold surroundings. This may also explain the relatively constant surface gradient (4-6°C) that was maintained between the head and air temperature. Unlike in the trunk region, where juvenile contour feathers begin to emerge around 100-120 days of age, the head region remains largely covered in natal down until close to the end of chick-rearing. In addition, consistently high rates of blood flow to the head region may be required to ensure cognitive development and maintain effective brain function (Rashotte et al. 1998). While we acknowledge the challenge of determining the exact cause of low surface temperatures throughout the early stages of chick development, we believe that the role of plumage in maintaining a lower body surface-to-environment thermal gradient is the most plausible interpretation of our results. While it is possible that the chicks may have employed local heterothermic responses to conserve energy early in ontogeny, studies have shown that wandering albatross chicks exhibit well developed homeothermy at about 30 days of age (Mougin 1970), i.e. some 120 days before the observed increase in trunk temperature (Fig. 4;

Fig. 5c). Early homeothermy is advantageous if resources are plentiful, since the reduction in energy expenditure associated with peripheral cooling is likely not conducive to efficient growth.

Feather moult is one of the most energetically costly processes in birds. Peripheral blood flow is increased as contour and wing feathers begin to develop, signalling the transition from natal down to juvenile plumage (Visser 1998). In some species, peak moult coincides with a doubling of basal metabolic rate (Lindström et al. 1993), representing a substantial increase in energy expenditure. The energy budget of birds during the moult is split such that over 70% of energy intake is used to cover the thermoregulatory costs associated with higher blood flow to the skin and increased biosynthesis during feather formation (Beltran et al. 2018). It follows, therefore, that during the transition from down to contour feathers, we expected increased surface temperature in the trunk region with chick age, associated with greater peripheral blood flow to supply nutrients and energy for feather formation. Our results supported this prediction, in that there was a marked increase in trunk temperature starting at 100-120 days of age. Thereafter, the increase in trunk temperature with chick age was broadly linear until fledging.

The extent to which newly-hatched chicks are able to regulate their body temperature varies across species and is influenced by their position on the altricial-precocial spectrum (Starck & Ricklefs 1998). Precocial chicks generally have a high thermogenic capacity, with some species achieving thermal independence within 24 hours of hatching (Visser 1998; Baarendse et al. 2007). The thermogenic response to cold of altricial chicks varies, but the development of competent endothermy is generally slower, and typically occurs several days after hatching (Ricklefs & Hainsworth 1968; Wegrzyn 2013). A decreasing gradient between surface temperature and ambient temperature with age coincides with the development of endothermy (Montevecchi & Vaughan 1989); therefore, as chicks mature and their ability to

regulate blood flow at the periphery increases, the surface temperature gradient is expected to decrease in un-feathered regions (eye, bill), where the effects of insulation on heat transfer are minimal. Our results support this prediction, with a marked decrease in the eye-region surface temperature gradient at ~120 days of age (Fig. 5e).

Unsurprisingly, our results show that the effects of weather on temperature gradients were more pronounced in uninsulated than insulated body regions. Wind speed, relative humidity and cloud cover all reduced eye surface temperature. Interactions between surface temperature gradients and weather parameters in uninsulated regions were strongly dependent on the age of the chick, weakening as the chicks matured. Eye surface temperature in particular showed high variation in response to relative humidity across the different plumage classes (i.e., ~6°C difference between chicks of 50-200 days of age at 50% humidity; Fig. 6b). This large difference presumably reflects the increased capacity for more effective temperature regulation in older chicks. Interactions between surface temperature gradients and environmental parameters were also dependent on the age of the chick for insulated regions, but not in a uniform manner across different age categories. When chicks are young, the drop in surface temperature with increasing relative humidity is indicative of the response to wetting of the plumage by rain or melting snow (Nye 1964). As chicks age, we expected that there would be less of an effect of relative humidity on surface temperatures due to the waterproofing properties of contour feathers (Nye 1964). However, our results do not support these predictions, suggesting that factors other than weather are involved in how surface temperature variation affects chicks throughout development in insulated body regions.

Modelling showed how heat loss was predicted to change with chick age, indicating that the sum of radiative and conductive heat loss increased 3-fold throughout development. When expressed as a heat flux (i.e., heat loss per unit surface area), there was an obvious change from a decreasing to an increasing trend starting around 150 days of age. Previous studies on

wandering albatross chicks found that the absolute resting metabolic rate (RMR) peaked (at 150% of adult metabolism) when chicks achieved maximum body mass in mid-winter and decreased close to fledging (Mabille et al. 2004). Studies of smaller species of albatrosses found absolute increases in resting metabolism with chick age but decreases in mass specific metabolic rate, from 5.0 Wkg^{-1} during the earliest part of linear growth to 3.5 Wkg^{-1} by the time chicks reached peak mass (Phillips et al. 2003). Our higher estimates may reflect the fact that we estimated heat loss for chicks in their natural habitat exposed to the full range of air temperature and wind speeds; conditions that can hardly be matched during measurements in a metabolic chamber.

In contrast to previous studies of chick RMR, the minimum predicted total heat loss from our model did not correspond to the maximum body mass of chicks, but continued to show an increase with age. Measured field metabolic rates (FMR) of wandering albatrosses (chicks and adults) using a number of different methods, range from 3.94 to 4.90 Wkg^{-1} (mean = 4.48), and estimates of RMR from 1.70 to 3.99 Wkg^{-1} (mean = 2.70) (reviewed by Teixeira et al. 2014). Dynamic Energy Budget (DEB) modelling by Teixeira et al. 2014 estimate FMR and RMR of adult wandering albatross to be 33.74 W (4.29 Wkg^{-1}) and 22.56 W (2.87 Wkg^{-1}), respectively. Thus, our estimates fall within the range of field measurements and modelled metabolic rates for growing wandering albatross chicks and adults. This is encouraging when considering that our heat loss model only considered heat loss by radiation and convection and did not take into account respiratory, other evaporative, and conductive heat loss, and did not consider heat gain by solar radiation. By modelling changes in heat loss with age, we provide insights into how total heat loss from the body is closely matched to changes in body surface temperature. Therefore, even if the basal rate of metabolism decreases with age, a combination of developmental changes in plumage, changes in behaviour and environmental conditions may serve to increase heat loss from different parts of the body. Moreover, feather growth and

increased activity to strengthen wing muscles during the later stages of development may increase peripheral blood flow, increasing the surface temperature distribution and therefore leading to higher heat loss before fledging.

5. Conclusions

Our study highlighted the effects of chick age and environmental conditions on surface temperature gradients across various body regions in wandering albatross chicks. Plumage development appeared to be an important driver of surface temperature gradients and heat loss in insulated body regions, probably because the moulting period is a time of increased thermoregulatory and other energetic demands across both avian and mammalian taxa (Lindström et al. 1993; Chaise et al. 2019). The dense plumage of wandering albatross chicks is an adaptation to cope with the rigours of their environment. However, if Antarctic warming leads to an increase in air temperatures, this may lead to thermal stress that requires channelling of resources from growth to heat dissipation, as observed in temperate study systems (e.g. Rodríguez & Barba 2016; Andreasson et al. 2018; Conradie et al. 2019). Climate change is also expected to bring increased frequency of heavy precipitation events and higher wind speeds (IPCC 2014). The direct effect of increased wetting and storm exposure may place greater, and potentially unmanageable thermoregulatory demands on wandering albatross chicks, and polar fauna more generally. Increasing wind speed at the poles may also affect the foraging efficiency of adults (Weimerskirch et al. 2012), affecting provisioning rates. In addition, chicks may suffer from the indirect impacts of anthropogenic climate change through alterations to ocean food web dynamics or decreased productivity (Hoegh-Guldberg & Bruno 2010), which may result in longer foraging trips by adults. Hence, climate change probably affects wandering albatross chick growth and thermoregulation both directly and indirectly via

changes to parental behaviour. These effects are likely exacerbated by increased anthropogenic disturbance in polar regions.

Predicting the responses of birds and mammals to forecasted changes in climatic conditions associated with greenhouse gas emissions presents a major challenge (Walther et al. 2002; Kiat et al. 2019). This work fills a gap in knowledge of temperature regulation in chicks with a long nestling stage that also experience severe climatic conditions. It therefore provides a foundation for further studies on the effects of environmental stressors during ontogeny that will determine the physiological responses of these polar animals to future changes in climate and resource abundance in their environment.

Acknowledgements

We thank Derren Fox and Peter Saunders at the British Antarctic Survey for assistance with collecting field data. The animal handling was approved by the British Antarctic Survey Ethics Committee (Ethics approval #1001) and carried out under permit from the Government of South Georgia and the South Sandwich Islands (Permit #2017/021). This work represents a contribution to the Ecosystems component of the British Antarctic Survey Polar Science for Planet Earth Programme, funded by the Natural Environment Research Council. The project was undertaken by David W. Stone in partial fulfilment of a MSci Zoology at the University of Glasgow. Thanks also to Lindsay Fergusson for GIS assistance. Andreas Nord was supported by the Birgit and Hellmuth Hertz Foundation / The Royal Physiographic Society of Lund (grant no. 2017-39034).

Declarations of interest

The authors declare that they have no conflict of interest.

References

Andreasson, F., Nord, A. & Nilsson, J-Å., 2018. Experimentally increased nest temperature affects body temperature, growth and apparent survival in blue tit nestlings. J. Avian Biol. 49, 1–14.

Baarendse, P.J.J., Debonne, M., Decuypere, E., Kemp, B. & Van Den Brand, H., 2007. Ontogeny of avian thermoregulation. World Poultry Sci. J. 63, 267–276.

Bates, D., Maechler, M., Bolker, B., & Walker, S., 2015. Fitting linear mixed-effects models using lme4. J. Stat. Softw. 67, 1–48.

Beltran, R.S., Burns, J.M., & Breed, G.A., 2018. Convergence of biannual moulting strategies across birds and mammals. Proc. R. Soc. B. 285, 20180318.

Blix, A.S., 2016. Adaptations to polar life in mammals and birds. J. Exp. Biol. 219, 1093-1105.

Bostwick, K., 2016. Feathers and Plumages, in: Lovette, I.J. & Fitzpatrick, J.W. (Eds.), Handbook of Bird Biology. Princeton University Press, New Jersey, pp 101-147.

Buchholz, R., 1996. Thermoregulatory role of the un-feathered head and neck in male wild turkeys. Auk 113, 310–318.

Chaise, L.L., McCafferty, D.J., Krellenstein, A., Gallon, S.L., Paterson, W.D., Théry, M., Ancel, A. & Gilbert, C., 2019. Environmental and physiological determinants of huddling behavior of molting female southern elephant seals (*Mirounga leonina*). Physiol. Behav. 199, 182-190.

Cilulko, J., Janiszewski, P., Bogdaszewski, M. & Szczygielska, E., 2012. Infrared thermal imaging in studies of wild animals. Eur. J. Wildl. Res. 59, 17-23.

Conradie, S.R., Woodborne, S.M., Cunningham, S.J. & McKechnie, A.E., 2019. Chronic, sublethal effects of high temperatures will cause severe declines in southern African arid-zone birds during the 21st century. Proc. Natl. Acad. Sci. U.S.A. 116, 14065–14070.

Davenport, J. & Macalister, H., 1996. Environmental conditions and physiological tolerances of intertidal fauna in relation to shore zonation at Husvik, South Georgia. J. Mar. Biol. Assoc. UK. 76, 985–1002.

Fox, J. & Weisberg, S., 2011. An R Companion to Applied Regression, second ed. Thousand Oaks California, Sage.

Gardner, J.L., Symonds, M.R.E., Joseph, L., Ikin, K., Stein, J., and Kruuk, L.E.B., 2016. Spatial variation in avian bill size is associated with humidity in summer among Australian passerines. Climate Change Responses 3, 1–11.

Gilbert, C., Le Maho, Y., Robertson, G., Naito, Y. & Ancel, A., 2006. Huddling behaviour in emperor penguins: dynamics of huddling. Physiol. Behav. 88, 479-488.

Gilbert, C., Le Maho, Y., Perret, M. & Ancel, A., 2007. Body temperature changes induced by huddling in breeding male emperor penguins. Am. J. Physiol. 292, 176–185.

Hammel, H.T., 1956. Infrared Emissivities of Some Arctic Fauna. J. Mammal. 37, 375–378.

Hoegh-Guldberg, O. & Bruno, J.F., 2010. The impact of climate change on the world's marine ecosystems. Science 328, 1523-1528.

Howell, T.R. & Bartholomew, G.A., 1961. Temperature Regulation in Laysan and Black-Footed Albatrosses. Condor 63, 185–197.

IPCC, 2014. Climate Change 2014: Synthesis Report. Contribution of Working Groups I, II and III to the Fifth Assessment Report of the Intergovernmental Panel on Climate Change [Core Writing Team, Pachauri, R.K. & Meyer, L.A. (eds.)]. IPCC, Geneva, Switzerland, 151 pp.

Irving, L. & Krog, J., 1955. Temperature of skin in the Arctic as a regulator of heat. J. Appl. Physiol. 7, 355-364.

Johansen, K. & Bech, C., 1983. Heat conservation during cold exposure in birds (vasomotor and respiratory implications). Polar Res. 1, 259-268.

Kiat, Y., Vortman, Y. & Sapir, N., 2019. Feather moult and bird appearance are correlated with global warming over the last 200 years. Nat. Commun. 10, 2540.

Kuznetsova, A., Bruun, P., & Bojesen Christensen, R. H., 2017. lmerTest: Tests in linear mixed effects models. R package version 2.0-32. Retrieved from https://CRAN.R project.org/package=lmerTest

Lindström, Å., Visser, G.H. & Daan, S., 1993. The energetic cost of feather synthesis is proportional to basal metabolic rate. Physiol. Zool. 66, 490-510.

Mabille, G., Boutard, O., Shaffer, S.A., Costa, D.P. & Weimerskirch, H., 2004. Growth and energy expenditure of Wandering Albatross *Diomedea exulans* chicks. Ibis. 146(1), 85–94.

Matuszko, D., 2012. Influence of the extent and genera of cloud cover on solar radiation intensity. Int. J. Climatol. 32, 2403–2414.

McCafferty, D.J., Gilbert, C., Paterson, W., Pomeroy, P., Thompson, D., Currie, J.I. & Ancel, A., 2011. Estimating metabolic heat loss in birds and mammals by combining infrared thermography with biophysical modelling. Comp. Biochem. Phys. A. 158(3), 337–345.

McCafferty, D.J., Gallon, S., and Nord, A., 2015. Challenges of measuring body temperatures of free - ranging birds and mammals. Anim. Biotelem. 3:33, 1–10.

Midtgård, U., 1983. Scaling of the Brain and the Eye Cooling System in Birds: A Morphometric Analysis of the *Rete Ophthalmicum*. J. Exp. Zool. 207, 197–207.

Monteith, J.L. & Unsworth, M.H., 1990. Principles of Environmental Physics (Vol. 2nd). Edward Arnold, London.

Montevecchi, W.A. & Vaughan, R.B., 1989. The Ontogeny of Thermal Independence in Nestling Gannets. Ornis. Scand. 20, 161–168.

Mougin, J.L., 1970. Observations cologiques sur les Grands Albatros (*Diomedea exulans*) de I'le de la Possession (Archipel Crozet). Oiseau et R.F.O. 40, 16-36.

Nye, P.A., 1964. Heat loss in wet ducklings and chicks. Ibis 106, 189-197.

Osvath, G., Daubner, T., Dyke, G., Fuisz, T.I., Nord, A., Penzes, J., Vargancsik, D., Vagasi, C.I., Vincze, O. & Pap, P.L., 2018. How feathered are birds? Environment predicts both the mass and density of body feathers. Funct. Ecol. 32, 701-712.

Ovstedal, D.O. & Lewis-Smith, R.I., 2001. Lichens of Antarctica and South Georgia: A Guide to their Identification and Ecology. Cambridge University Press, Cambridge.

Phillips, R.A., Green, J.A., Phalan, B., Croxall, J.P. & Butler, P.J., 2003. Chick metabolic rate and growth in three species of albatross: a comparative study. Comp. Biochem. Phys. A. 135(1), 185–193.

Phillips, R.A. & Hamer, K.C., 2000. Postnatal development of northern fulmar chicks *Fulmarus glacialis*. Physiol. Biochem. Zool. 73, 597-604.

Ponganis, P.J., Van Dam, R.P., Levenson, D.H., Knower, T., Ponganis, K.V. & Marshall, G., 2003. Regional heterothermy and conservation of core temperature in emperor penguins diving under sea ice. Comp. Biochem. Phys. A. 135, 477-487.

Price, E.R. & Dzialowski, E.M., 2018. Development of endothermy in birds: patterns and mechanisms. J. Comp. Physiol. B. 188, 373-391.

R Development Core Team, 2018. R: A language and environment for statistical computing. 3.5.1 Ed. Vienna, Austria: R Development Core Team.

Rashotte, M.E., Pastukhov, I.F., Poliakov, E.L. & Henderson R,P., 1998. Vigilance states and body temperature during the circadian cycle in fed and fasted pigeons (*Columbia livia*). Am. J. Physiol. 275, R1690 – R1702.

Ricklefs, R.E., 1979. Adaptation, Constraint, and Compromise in Avian Postnatal Development. Biol. Rev. 54, 269-290.

Ricklefs, R.E., 1989. Adaptation to cold in bird chicks, in: Bech, C. & Reinertsen, R.E. (Eds.), Physiology of Cold Adaptation in Birds. Plenum Press, New York, pp 329-338.

Ricklefs, R.E. & Hainsworth, F.R., 1968. Temperature regulation in nestling cactus wrens: The development of homeothermy. Condor 70, 121-127.

Rodríguez, S. & Barba, E., 2016. Nestling growth is impaired by heat stress: an experimental study in a Mediterranean great tit population. Zool. Stud. 55, 40.

Schneider, C.A., Rasband, W.S. & Eliceiri, K.W., 2012. NIH Image to ImageJ: 25 years of image analysis. Nat. Methods. 9, 671-675.

Schraft, H.A., Whelan, S. & Elliott, K.H., 2019. Huffin' and puffin: seabirds use large bills to dissipate heat from energetically demanding flight. J. Exp. Biol. 222, 2017-2019.

Starck, J.M. & Ricklefs, R.E., 1998. Avian Growth and Development: Evolution within the Altricial-Precocial Spectrum. Oxford University Press, Oxford.

Strother, S.L., Salzmann, U., Roberts, S.J., Hodgson, D.A., Woodward, J., Van Nieuwenhuyze, W., Verleyen, E., Vyverman, W. & Moreton, S.G., 2015. Changes in Holocene climate and the intensity of Southern Hemisphere Westerly Winds based on a high-resolution palynological record from sub-Antarctic South Georgia. Holocene 25, 263–279.

Symonds, M.R.E. & Tattersall, G.J., 2010. Geographical Variation in Bill Size across Bird Species Provides Evidence for Allen 's Rule. Am. Nat. 176, 188–197.

Teixeira, C., Sousa, T., Marques, G.M., Domingos, T., and Kooijman, S.A., 2014. A new perspective on the growth pattern of the wandering albatross (*Diomedea exulans*) through DEB theory. J. Sea Res. 94, 117–127.

Tickle, P.G. & Codd, J.R., 2019. Thermoregulation in rapid growing broiler chickens is compromised by constraints on radiative and convective cooling performance. J. Therm. Biol. 79, 8–14.

Visser, G.H., 1998. Development of Temperature Regulation, in: Starck, J.M. & Ricklefs, R.E. (Eds.), Avian Growth and Development: Evolution within the Altricial-Precocial Spectrum. Oxford University Press, Oxford, pp 117-156.

Visser, G.H. & Ricklefs, R.E., 1995. Relationship between body composition and homeothermy in neonates of precocial and semiprecocial birds. Auk 112, 192–200.

Walther, G., Post, E., Convey, P., Menzel, A., Parmesan, C., Beebee, T.J.C., Fromentin, J., Hoegh-Guldberg, O. & Bairlein, F., 2002. Ecological responses to recent climate change. Nature 416, 389-395.

Wegrzyn, E., 2013. Resource allocation between growth and endothermy allows rapid nestling development at low feeding rates in a species under high nest predation. J. Avian Biol. 44, 383-389.

Weimerskirch, H., Louzao, M., de Grissac, S. & Delord, K., 2012. Changes in wind pattern alter albatross distribution and life-history traits. Science 335, 211-214.

Wharton, D.A., 2002. Life at the Limits: Organisms in Extreme Environments. Cambridge University Press, Cambridge.

Winder, L.A., White, S.A., Nord, A., Helm, B. & McCafferty, D.J., 2020. Body surface temperature responses to food restriction in wild and captive great tits (*Parus major*). J. Exp. Biol. In press.

Zuur, A.F., Ieno, E.N. & Smith, G.M., 2007. Analysing Ecological Data. Springer, New York.

Table 1. Wandering albatross chick surface temperatures ($T_{surface}$), surface temperature-air gradients ($T_{surface} - T_{air}$), and environmental variables recorded throughout this study. Values are the mean ± SE with the range in parentheses.

$T_{surface}$ (°C)	Mean ± SE (range)
Eye	22.6 ± 0.2 (11.6 - 31.5)
Bill	10.7 ± 0.3 (1.1 - 26.9)
Head	6.4 ± 0.2 (-1.5 - 18.8)
Trunk	5.1 ± 0.3 (-5.0 - 25.2)
$T_{surface} - T_{air}$ (°C)	
Eye	20.8 ± 0.2 (11.0 - 28.7)
Bill	9.0 ± 0.3 (0.7 - 23.8)
Head	4.7 ± 0.1 (-1.5 - 12.4)
Trunk	3.4 ± 0.2 (-3.6 - 17.2)
Environmental Variable	
Wind Speed (m/s)	3.9 ± 0.1 (0.0 - 14.0)
Air Temperature (°C)	1.7 ± 0.2 (-5.1 - 9.3)
Relative Humidity (%)	83.2 ± 0.7 (54 - 100)
Cloud Cover (%)	81.9 ± 1.6 (10 - 100)

Table 2. Test statistics, degrees of freedom (Satterthwaite approximation) and *P*-values for final models of surface temperature gradients in response to age and environmental variables in wandering albatross chicks during the austral winter on Bird Island, South Georgia.

Parameter	Estimate	SE	d.f.	*t*	*P*
$T_{eye} - T_{air}$ (°C)					
Age (d)	-0.09	0.02	299	-5.54	<0.0001
Wind (m/s)	-0.73	0.17	299	-4.26	<0.0001
Relative Humidity (%)	-0.13	0.03	299	-3.76	<0.0001
Cloud (%)	-0.03	0.01	299	-2.07	<0.001
Age (d) × Wind (m/s)	0.003	0.001	299	2.93	0.04
Age (d) × Relative Humidity (%)	0.0005	0.0002	299	2.56	0.004
Age (d) × Cloud (%)	0.0002	0.0001	299	1.98	0.01
$T_{bill} - T_{air}$ (°C)					
Age (d)	-0.01	0.004	284	-3.22	0.001
Relative Humidity (%)	-0.1	0.02	291	-4.19	<0.0001
Cloud (%)	-0.02	0.01	282	-2.09	0.04
$T_{head} - T_{air}$ (°C)					
Age (d)	0.04	0.06	292	0.59	0.55
Age^2 (d)	-0.0001	0.0002	292	-0.55	0.59
Wind (m/s)	-0.18	0.05	288	-3.75	0.002
Relative Humidity (%)	0.11	0.06	294	1.94	0.05
Cloud (%)	-0.05	0.03	286	-1.71	0.09
Age (d) × Relative Humidity (%)	-0.002	0.0008	293	-2.31	0.02

Age (d) × Cloud (%)	0.001	0.0004	286	2.49	0.01
Age^2 (d) × Relative Humidity (%)	<0.0001	<0.0001	294	2.31	0.02
Age^2 (d) × Cloud (%)	<-0.0001	<0.0001	288	-2.74	0.006
$T_{trunk} - T_{air}$ (°C)					
Age (d)	-0.1	0.05	299	-1.97	0.05
Age^2 (d)	0.0005	0.0001	299	3.45	0.0006
Posture (Standing)	0.82	0.3	299	2.71	0.007
Wind (m/s)	-0.19	0.07	299	-2.84	0.005
Relative Humidity (%)	0.05	0.04	299	1.39	0.16
Cloud (%)	-0.09	0.04	299	-2.37	0.02
Age (d) × Relative Humidity (%)	-0.0005	0.0002	299	-2.03	0.04
Age (d) × Cloud (%)	0.001	0.0005	299	2.37	0.02
Age^2 (d) × Cloud (%)	<-0.0001	<0.0001	299	-2.28	0.02

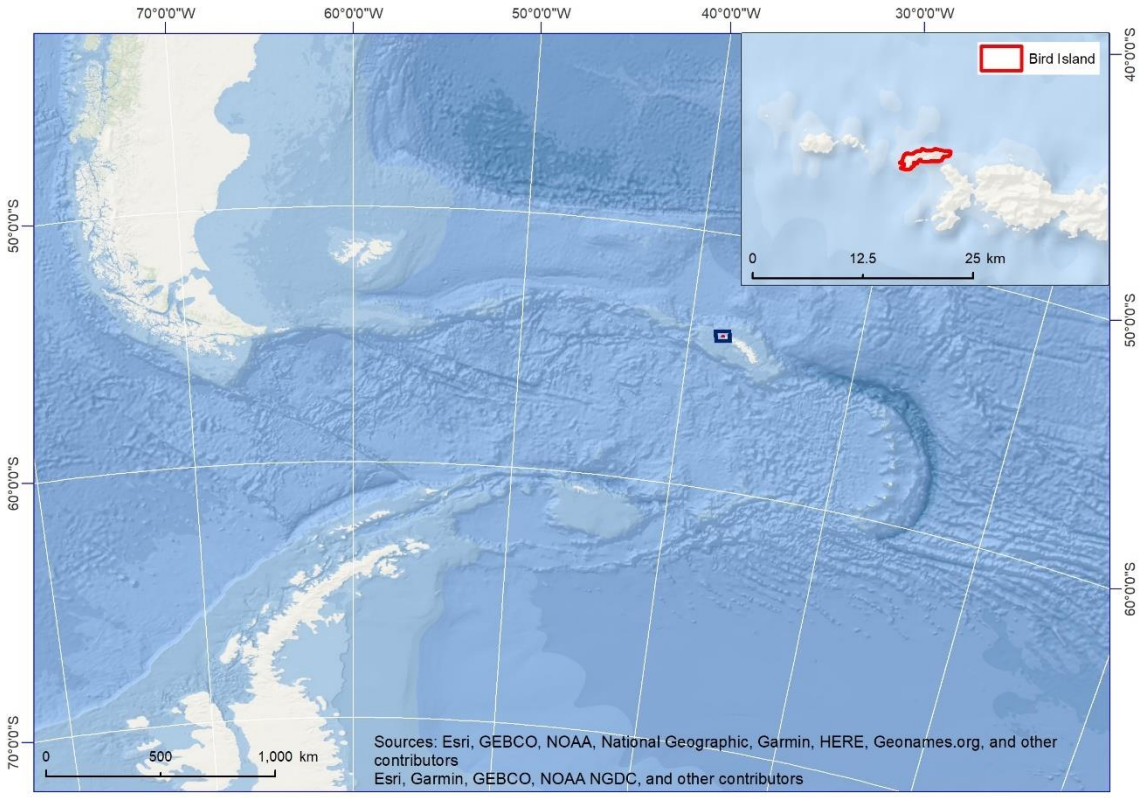

Fig. 1. Map of the study site, Bird Island, South Georgia (54° 00′ S, 38° 03′ W), in the south Atlantic Ocean.

0: 0% **1: >0% - 25%** **2: >25% - 50%**

3: >50% - 75% **4: >75%**

Fig. 2. Five level (0-4) plumage classification of wandering albatross chicks on Bird Island, South Georgia. All 19 individuals in the study were assigned a plumage classification at each of the 25 sessions based on the percentage cover of teleoptile (juvenile) plumage.

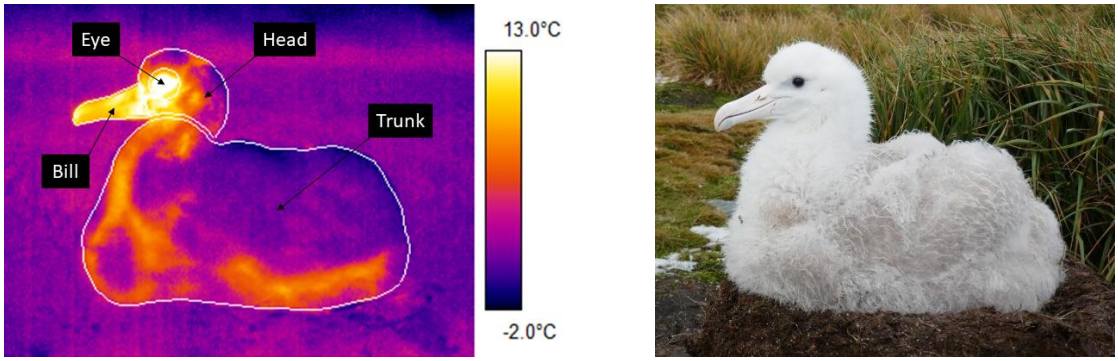

Fig. 3. Thermal (left) and visual image (right) of an 8-week old wandering albatross chick on Bird Island, South Georgia. Thermal images were obtained using an E300 FLIR thermal camera and analysed using ThermaCAM Researcher Pro 2.10. The images were adjusted for variation in air temperature, relative humidity, and distance from object, after which we traced the outline of the eye, bill, trunk and head regions and extracted surface temperature data from the fitted shapes.

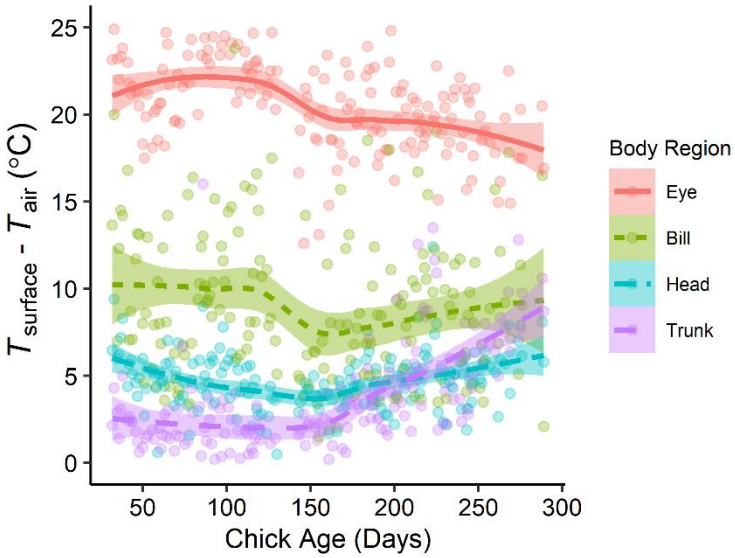

Fig. 4. Changes in the maximum surface temperature gradient of the eye region and mean surface temperature gradients of the bill, head and trunk regions with age in wandering albatross chicks on Bird Island, South Georgia. Trend lines are fitted using the LOESS (Locally Estimated Scatterplot Smoothing) method, with shaded regions indicating ± 95% confidence intervals.

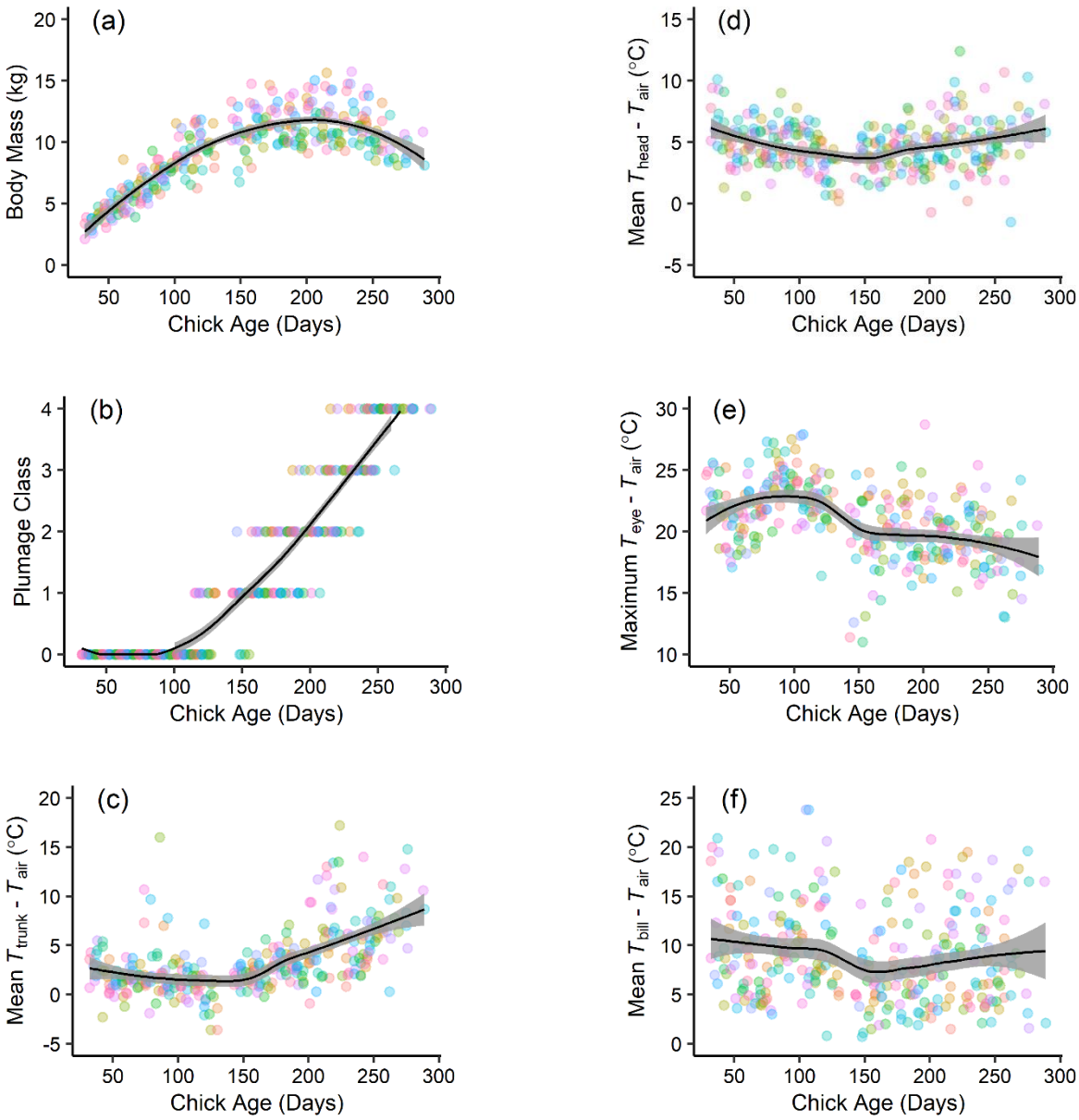

Fig. 5. Changes with age of wandering albatross chicks in body mass (a), plumage moult class (b), mean surface temperature gradient in the trunk region (c), mean surface temperature gradient in the head region (d), maximum surface temperature gradient in the eye region (e) and mean surface temperature gradient in the bill region (f). For plumage classification, see the main text and Fig. 2. Trend lines on all plots are fitted using the LOESS (Locally Estimated Scatterplot Smoothing) method ± 95% confidence intervals. Individual chicks are plotted using different point colours.

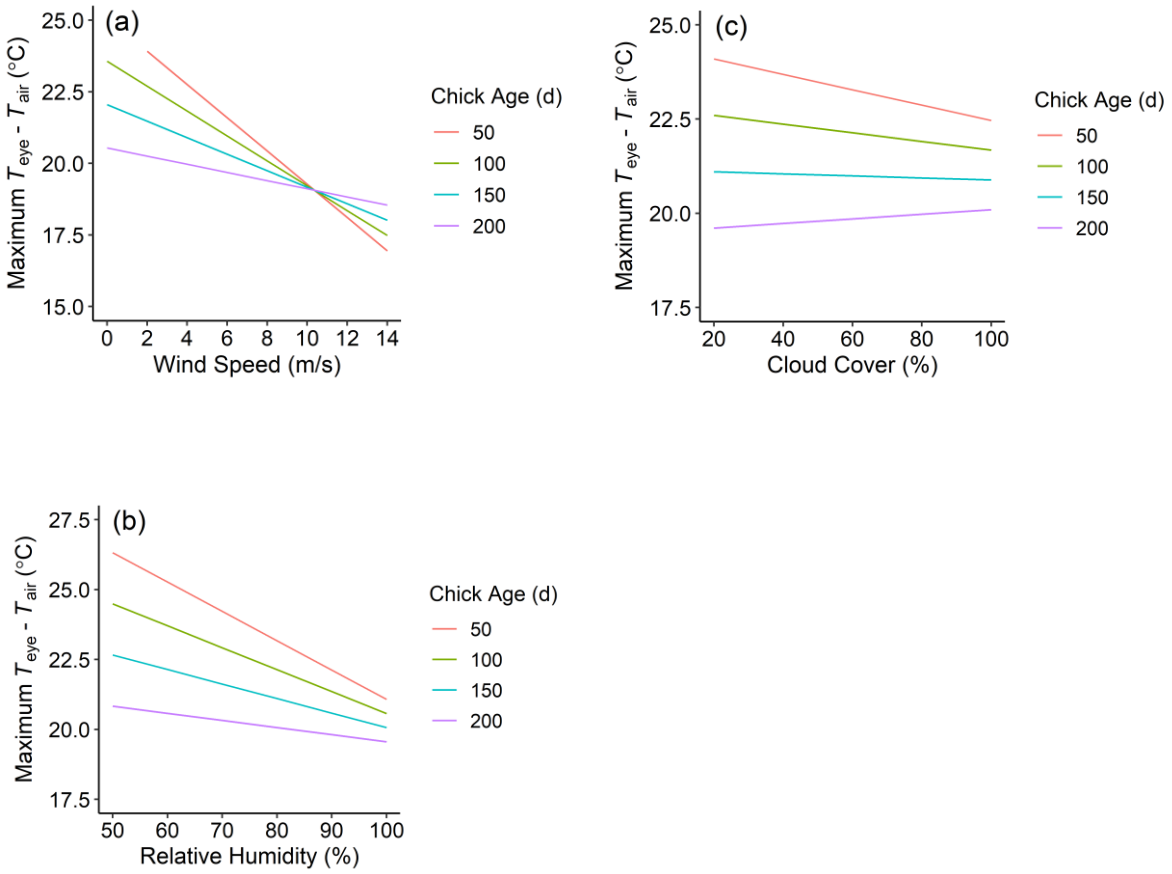

Fig. 6. Estimated marginal means for the interacting effects of age and weather conditions on eye region surface temperature gradients in wandering albatross chicks on Bird Island, South Georgia, for wind speed (a), relative humidity (b), and cloud cover (c).

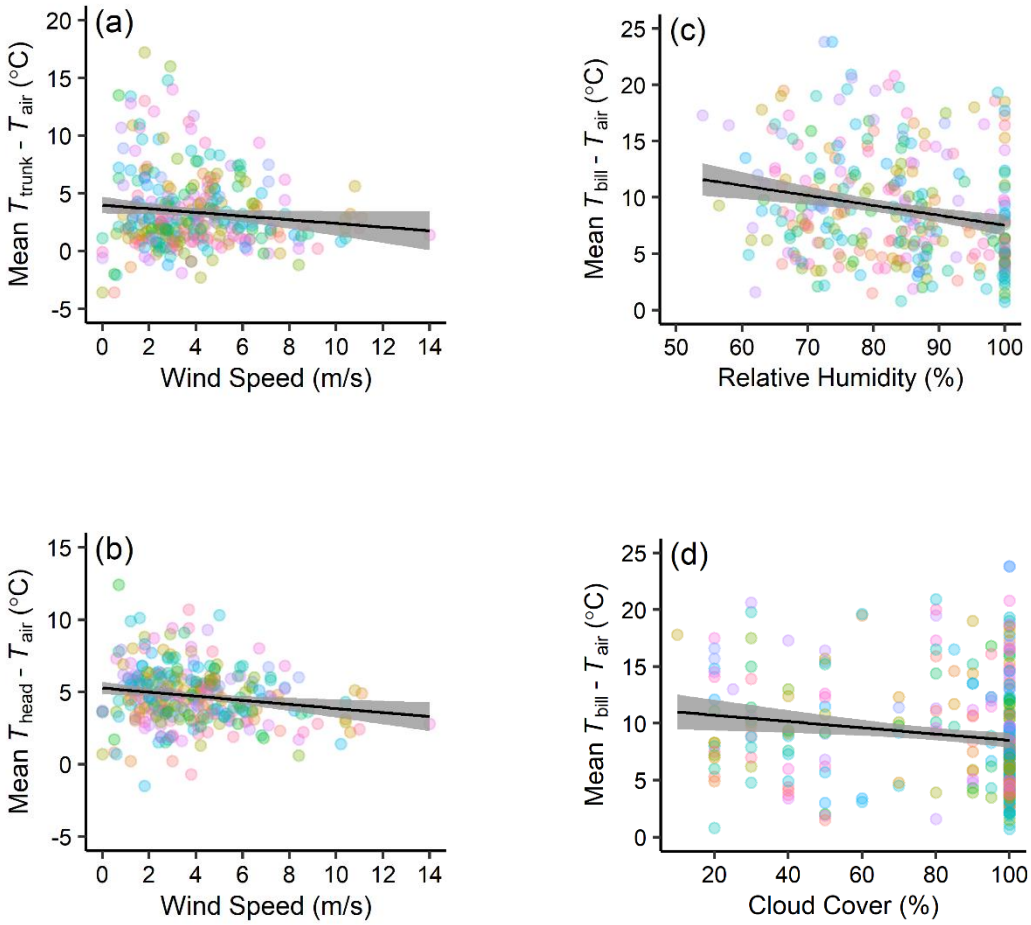

Fig. 7. Surface temperature gradient changes in the insulated trunk (a) and head (b) regions in response to wind speed, and in the uninsulated bill region in response to relative humidity (c) and cloud cover (d), for wandering albatross chicks on Bird Island, South Georgia. Trend lines on all plots are fitted using the LM (Linear Model) method ± 95% confidence intervals. Each point colour represents repeated measurements from the same chick.

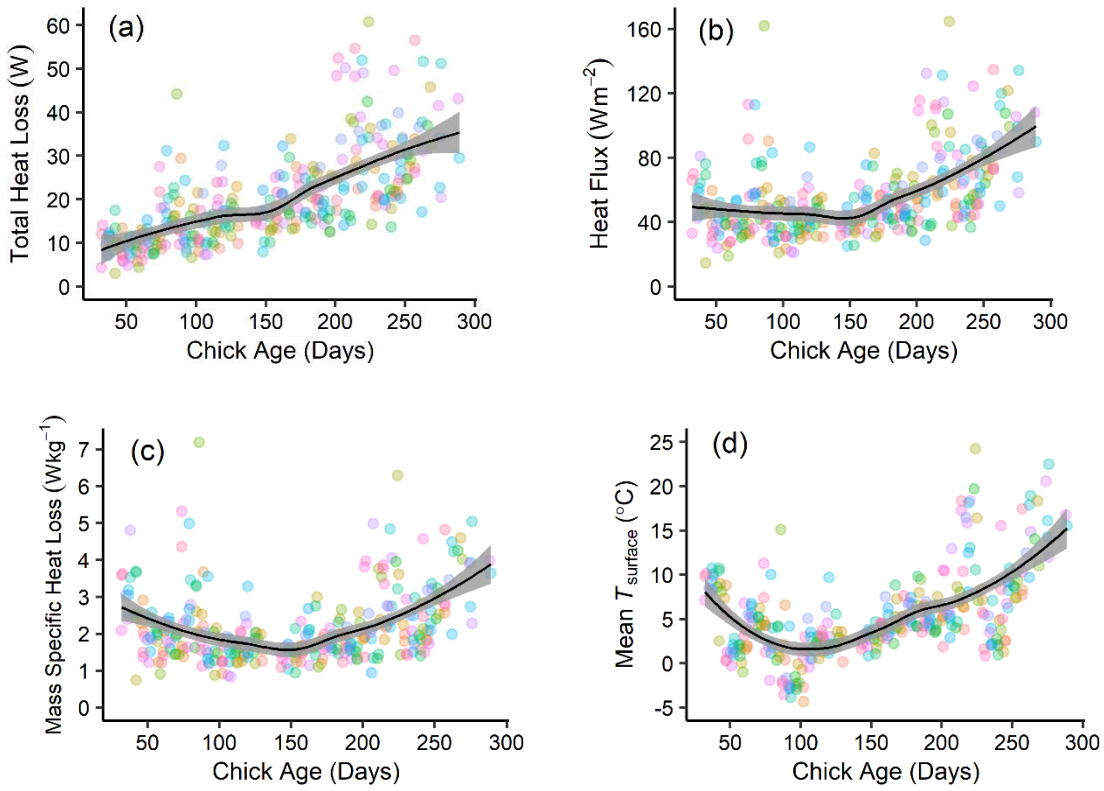

Fig. 8. Modelled changes in total heat loss (a), heat flux in Wm^{-2} (b), mass specific heat loss in Wkg^{-1} (c) and mean surface temperature in ^{o}C (d) with age in wandering albatross chicks on Bird Island, South Georgia. Trend lines on all plots were fitted using the LOESS (Locally Estimated Scatterplot Smoothing) method ± 95% confidence intervals. Individual chicks are plotted using different point colours.

Supplementary material

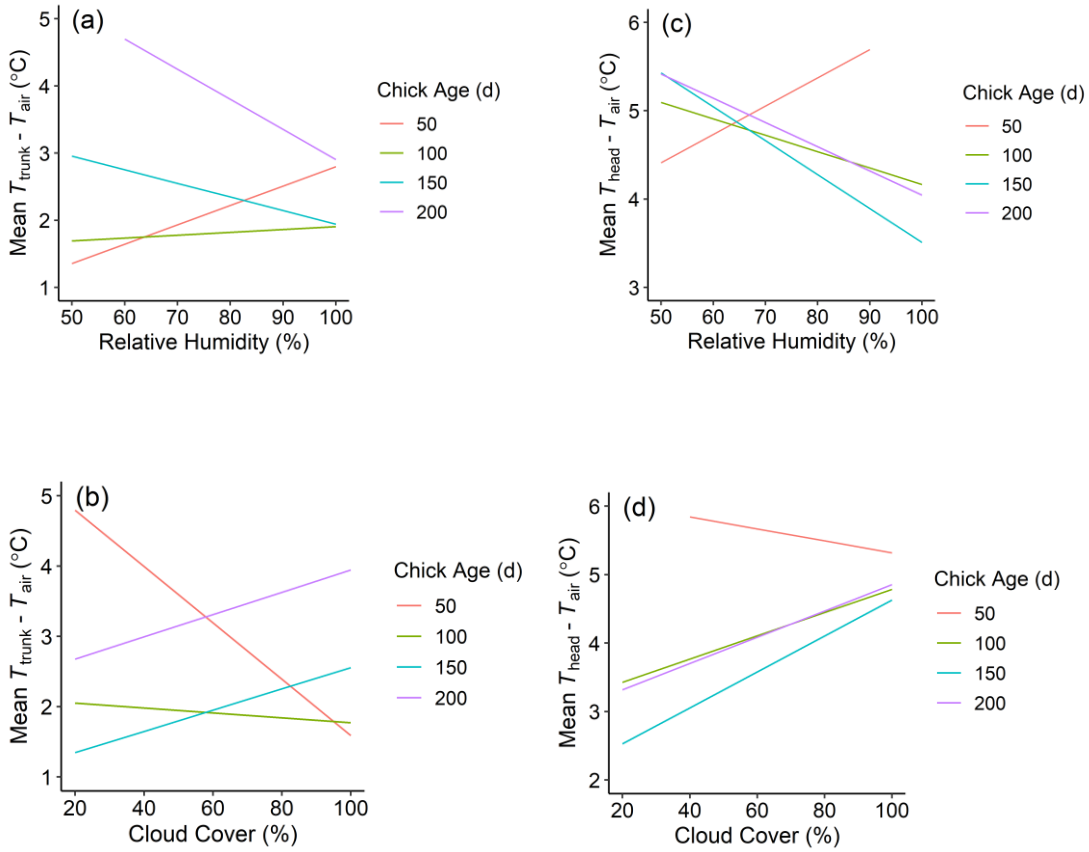

Fig. S1. Estimated marginal means in wandering albatross chicks on Bird Island, South Georgia for the effect of the interactions between age and weather conditions on trunk surface temperature gradients for relative humidity (a) and cloud cover (b); and on head surface temperature gradients for relative humidity (c) and cloud cover (d).

Table S1. Likelihood ratios (LRT) and *P*-values for excluded terms in the models of variation in surface temperature gradients in response to age and environmental variables in wandering albatross chicks during the austral winter on Bird Island, South Georgia.

Parameter	**LRT**	***P***
$T_{eye} - T_{air}$ **(°C)**		
Posture	0.18	0.67
Age^2 (d)	0.02	0.89
Age^2 (d) × Relative Humidity (%)	3.78	>0.05
Age^2 (d) × Cloud (%)	3.67	0.06
Age^2 (d) × Wind (m/s)	2.69	0.1
$T_{bill} - T_{air}$ **(°C)**		
Posture	2.59	0.11
Wind (m/s)	1.66	0.2
Age^2 (d)	0.95	0.33
Age (d) × Relative Humidity (%)	2.05	0.15
Age (d) × Wind (m/s)	0.54	0.46
Age (d) × Cloud (%)	0.42	0.51
Age^2 (d) × Wind (m/s)	1.49	0.22
Age^2 (d) × Cloud (%)	0.81	0.37
Age^2 (d) × Relative Humidity (%)	0.51	0.48
$T_{head} - T_{air}$ **(°C)**		
Posture	1.9	0.17
Age (d) × Wind (m/s)	0.11	0.74
Age^2 (d) × Wind (m/s)	2.22	0.14

$T_{trunk} - T_{air}$ (°C)		
Age (d) × Wind (m/s)	3.83	>0.05
Age^2 (d) × Relative Humidity (%)	3.77	>0.05
Age^2 (d) × Wind (m/s)	3.72	>0.05